Synthesis and characterization of ZnO nanoparticles for modifying thermal and mechanical properties of industrial substrates

Anjana S. Desai[1], Aparna Ashok[1], Vaishnavi V. Dabir[2], Habib M. Pathan[3], Brajesh Pandey[4], and Neeru Bhagat[1,*]

[1] *Department of Applied Science, Symbiosis Institute of Technology, Symbiosis International (Deemed) University (SIU), Pune 412115, India*

[2] *Department of Civil Engineering, Symbiosis Institute of Technology, Symbiosis International (Deemed) University (SIU), Pune 412115, India*

[3] *Department of Physics, Savitribai Phule Pune University (SPPU), Pune 411007, India*

[4] *Indian National Science Academy, Bahadur Shah Zafar Marg, New Delhi 110002, India*

ABSTRACT

In this experimental study, zinc oxide nanoparticles (ZnO-NPs) are synthesized using *Moringa oleifera* extract and calcined at 400 °C. These biologically synthesized ZnO-NPs were mixed in 1:1 proportion with organic (oil) and quasi-organic (varnish) binder separately. These mixtures were individually coated on three substrates: paper, wood, and fabric (P, W, and F). The effect of the coating of NPs on the mechanical and thermal properties of the substrate was observed. XRD investigation revealed the formation of a wurtzite structure of synthesized NPs with a crystallite size of 28 nm. The morphology of ZnO-NPs, uncoated and coated P, W, and F substrates were studied by field emission scanning electron microscopy (FESEM). Our studies reveal that adding ZnO-NPs improved the fire resistance property of the materials. It also shows a measurable increase in the materials' tensile strength by adding ZnO-NPs.

1 Introduction

Many remarkable physical, chemical, and biological properties emerge in materials at the nanoscale. Engineered nanomaterials, especially metals and metal-oxide NPs are fabricated and designed for specific purposes or applications [1]. Due to their unique physical and chemical properties, they are highly in demand in the biomedical and industrial sectors [2–4]. Emerging material like carbon-based nanomaterials, nanocomposites, metals and alloys, biological nanomaterials, nano-polymers, nano-glasses, and nano-ceramics has been extensively used in the production line [5–9]. Though these materials are extensively used, some limitations hinder their further use in industries. The drawbacks associated are mainly in the preparation routes, cost, health impact, and environmental concerns [10–12]. The synthesis process mostly involves

Address correspondence to E-mail: neerubhagat@hotmail.com

expensive physical and chemical ways requiring highly sophisticated equipment. Maintaining the temperature and pressure conditions and involving toxic chemicals is crucial. The eco-friendly and cost-effective route makes biological synthesis a better alternative to conventional synthesis [13, 14]. Biologically prepared NPs like Ag, Au, Pt, ZnO, CuO etc., are mostly applicable in cosmetics, medicines, and in health-related devices due to their non-toxic behavior [15]. ZnO-NPs are widely used due to their broad range of characteristics, such as excellent electrical, optical, and chemical properties. Yet very few reported works use ZnO in technological developments [16]. Manufacturing industries fabricate various materials in an exponential trend. Research and development sectors intended to improve the properties of the materials by either incorporating the NPs or coating them on the substrates to enhance their mechanical strength, load-bearing capacity, UV retardation, flame retardations etc. [17, 18]. They are even utilized efficiently in manufacturing sectors like textile and paper pulp [19, 20]. The coating of NPs to the substrate needs a stronger adhesion, and organic or quasi-organic binders can achieve that. Considering sustainability, using organic binders can be a better solution [21].

Coating of NPs on different substrates has been attempted in various ways by research around the globe. Wong et al. attached the NPs to the fabrics using the padder technique with the help of rollers. It is observed that water repellence, soil resistance, wrinkle resistance, anti-bacterial property, anti-static and UV protection, flame retardation, and dye ability were improved in the coated fabric [22]. Radu Olar used nanomaterials (NMs) in the construction industries. The incorporation of NPs has specially developed structural concrete, real-time structural monitoring, coatings and paintings, and thermal insulations [23]. Monica J. Hanus et al. reported that the addition of TiO_2, Al_2O_3, ZrO_2, Fe_2O_3, SiO_2, SnO_2 nanoparticles and other metal oxides containing nano-clays used to modify the properties of concrete in terms of structural health monitoring, sensing devices, antimicrobial surfaces and in self-cleaning surfaces [24]. Fukugai-chi et al. modified the surface property of nano-TiO_2 coated paper in terms of dynamic elastic and viscosity modulus [25].

Nano-based treatments offer new opportunities to enhance wood, paper, and fabric attributes more effectively for different applications. Recent years have witnessed modifying wood, paper, and fabric by integrating inorganic metal oxides and organic binders, a novel approach to making value-added goods [26, 27]. New functional nanocomposite materials include hybrid ones covered in organic binders. Metal oxide nanomaterial, organic binder, and these hybrid components combine physically or chemically to provide synergistic effects that result in improved thermal and mechanical stability. The formation of charcoal, water, and other low-molecular-weight compounds can be increased by metal oxide NPs by decreasing the development of flammable volatiles [27, 28]. This impacts the kinetics of thermal degradation and the pyrolysis behavior of fibers, enhancing the effectiveness of intumescent fire retardants [28]. The commercialization of products requires easy synthesis of NPs and improved properties of the coated substrates like mechanical, antimicrobial thermal properties, etc. [29, 30]. This paper attempts to compare various substrates with green-synthesized ZnO-NPs in the presence of an organic and quasi-organic binder.

2 Materials and methods

Zinc nitrate hexahydrate ($Zn(NO_3)_2 \cdot 6H_2O$) for preparation of NPs was purchased from Sigma-Aldrich, and the *Moringa oleifera* leaves were collected from the local village. All the aqueous solutions were prepared in double-distilled water (DDW). The phytochemical compounds like vitamins, flavonoids, and phenolic acid in the Moringa oleifera are the biologically active ingredient that is vital in reducing the zinc salt into its NPs. The organic binder, namely linseed oil and quasi-organic binder i.e., varnish with natural resin, were purchased from local vendors.

The quasi-organic varnish was purchased from Natural Earth Paint which uses plant-based preservation components. The organic binder and the linseed oil were purchased from SV AGROFOOD. A genus Linum and family Linaceae member is flax (Linum usitatissimum). Linseed oil is extracted from nearly all of the domestically produced flaxseed.

3 Preparation of the moringa leaf extract

Clean and dried 25 g leaves of *Moringa oleifera* were immersed and boiled with the help of a magnetic stirrer in 100 ml of DDW at 60 °C. After cooling at room temperature, the mixture was filtered through

Whatman filter paper. The collected *Moringa oleifera* extract was stored in a refrigerator at 4 °C for further use.

4 Synthesis of ZnO-NPs through biological route

About 0.5 M of zinc nitrate hexahydrate was dissolved in 50 ml of DDW and kept on a magnetic stirrer till a clear solution was observed. The 50 ml of the above-prepared extract was added into the aqueous zinc nitrate solution and held for continuous stirring at 90 °C. This method has been modified from an earlier work by Bhagat et al., [31]. After completion of the reaction, the precipitate was collected and centrifuged. To remove the impurities, the precipitate was repeatedly washed with DDW and dried overnight in a hot air oven at 80 °C. Finally, the dried powder was calcined at 400 °C for 2 h.

5 Deposition of ZnO-NPs on the substrates

The most common techniques used for coating the substrates are spraying, transfer printing, washing, rinsing, dip-coating, and padding. Out of all, the most facile and economical technique widely used is the dip-coating method. It deposits the NPs on the substrates such as metallic, ceramic, polymer films, fibrous materials, etc.

All the substrates (P, W and F) were cleaned with water to remove the dust and dried at room temperature. The ZnO-NPs were dispersed in (1:1) proportions in the two different binders i.e., oil and varnish, ultrasonicated for 30 min, and applied on all three substrates in the presence of two different binders using a dip coating process. Once the coating was done, the samples were dried at room temperature.

6 Characterization techniques

Powder X-ray diffraction (P-XRD) is a rapid analytical technique primarily used to determine and confirm the crystal structure of ZnO-NPs. The most common target material for diffraction is copper with Cu Kα radiation of wavelength 1.5406 Å. The XRD measurement was conducted on Bruker D8 Advance

X-ray Diffractometer operated at 40 KV, and samples were scanned in the range of (2θ) 20– 90° at room temperature. The UV-Vis spectroscopy of ZnO-NPs was carried out using JASCOV-67 spectrometer in the wavelength range 800–200 nm. The UV-Visible absorption spectra of ZnO-NPs are shown in Fig. 3. FEI Nova Nano SEM 450 scanning electron microscope was used to study the morphology of prepared ZnO-NPs samples. Also, the FESEM was used to confirm the coating of NPs on the different substrates.

7 Flame retardation or flammability test

The flammability test is used to determine the relative rate of burning of self-supporting plastics, which are polyethylene resin of the high-density group (polypropylene, polyvinyl chloride etc.). The flammability is determined by ASTM D6413 method. ASTM D6413 is a standard test method to evaluate the flame resistance against electric arc and flash fire hazards. In this test, the samples are placed either horizontally or vertically in the test chamber. Then the flame from the Bunsen burner is applied for a specific time. Finally, the measurement of the time or distance for which flame propagates is recorded. In the case of a vertical flammability test, a material is observed for the length of time it burns after the igniting flame is removed, how much of the specimen burns, and whether or not it drips flaming particles. Data collected is of time taken until the flame extinguishes itself.

After-flame when the test specimen continues to flame after the flame source has been removed is known as the after-flame test,

After-glow when the test specimen continues to glow after removing the flame source is known as the after-flame test.

As the test method is ideal for 2D laminas (e.g. paper, fabric etc.) and not 3D structures such as wood, visual observation was noted after devising an in-house setup on the same principles and recording the time of after-flame and after-glow charring for wood in coated and non-coated form. The samples on which the test was carried on different substrates and are mentioned as bare paper (P), bare wood (W), bare fabric (F) and coated with ZnO NPs and binders (Oil and Varnish) as PZO, WZO, FZO, PZV, WZV and FZV.

8 Tensile strength test

The tensile test is one of the most important parameters for defining material strength. Determination of the maximum force that a material can sustain before it starts to deform plastically (yield strength) or the load at which the material breaks (tensile strength) is determined in this test. This test can also be used to calculate the elongation at break (fracture strain) for an elastic or elastoplastic material. The tensile test of wood was determined using (Universal Testing Machine) UTM of 50 kN capacity using the test method of ISO 10319:1993. The UTM has two cross heads, out of which one end is fixed, and the other is moving, which can be controlled by the operator. Fixing of flat jaws was ensured to hold the specimen in the crossheads. The specimen was then placed between the grips. The tension was gradually applied by controlled pulling action of the jaws on the specimen. The tension value at the failure of the specimen was observed in the case of bare wood (W), wood coated with ZnO NPs as WZ in the presence of Oil (O) and Varnish (V) as a binder. Tensile testing of the 2D laminas made up of paper (P), and fabric (F) substrates in bare form and in the form coated with ZnO NPs as PZ and FZ were tested on a setup devised in-house on the principle of ISO 10319:1993. The developed setup is shown in Fig. 1. As shown in Fig. 1, the setup consists of a top horizontal arm fixed on the top position, allowing for the insertion of the 2D lamina. The lower vertical arm consists of a clamp jaw that holds the 2D lamina, adding weights manually to apply tension to the specimen. The weights of 100 gms and 200 gms can be added into the screw gradually, and an observation time of 10 s is allowed to observe any visual elongation and the possibility of a tear. Once the 2D lamina
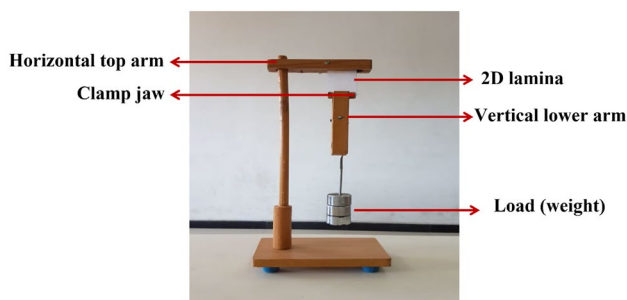
sustains the loading for the observation time, more weight is added and held for the observation time. The weight at which the tear occurs in the observation time is noted and the elongation of fibers is recorded manually using a ruler. The readings of modulus of elasticity can be determined as the ratio of stress to strain, where stress is the weight at failure divided by the cross-sectional area of the 2D lamina.

9 Result and discussion

9.1 Structural properties

Using an X-ray diffractometer, the P-XRD analysis was performed on biologically synthesized ZnO-NPs. The powder XRD pattern is shown in Fig. 2. The pattern matched the JCPDS file number (36-1451), and the peaks were indexed. The Scherrer formula,

$$D = \frac{K\lambda}{\beta \cos\theta}$$

The crystallite size was estimated using the fundamental Scherrer formula [32, 33], where D is the average crystallite size, λ (0.15406 nm) is the x-ray wavelength, β is the width of the X-ray peak on the 2θ axis (typically measured as the full width at half maximum (FWHM)),θ is the Bragg angle. K is the Scherrer constant usually close to 1. The value of K used here is 0.9, as used in our previous publication [31]. β is

Fig. 1 Setup developed in-house or tensile strength testing of 2D-Lamina
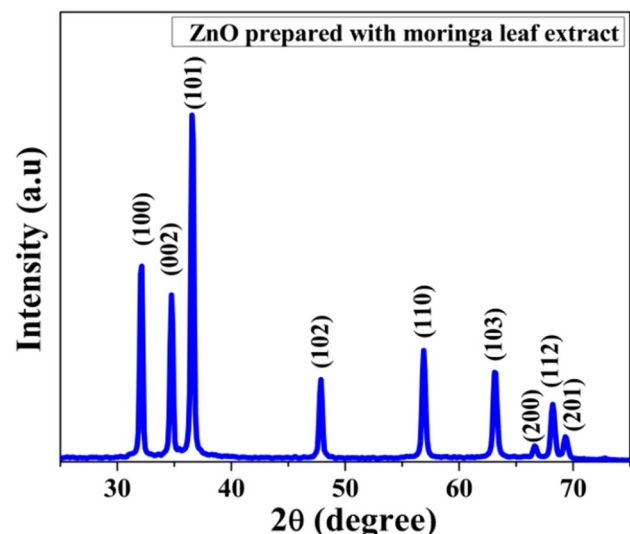

Fig. 2 XRD pattern of biologically synthesized ZnO-NPs

influenced by the size distribution and crystallite form, as well as by the diffraction line indices [33, 34].

The Miller indices of the various planes are (100), (002), (101), (102), (110), (103), (200), (112), (201) and (202). The diffraction peaks of the ZnO-NPs are indexed, corresponding to the hexagonal wurtzite structure of zinc oxide. The average crystallite size (D) was found to be 28 nm. The sharp and fine peaks represent the pure crystalline nature of the NPs. The intense peak of (101) for zinc-oxide nanomaterial exhibits anisotropic behavior [35–37].

9.2 Optical properties

The optical characteristics of ZnO-NPs were studied using UV–Visible spectroscopy, and it showed an absorbance peak at 359 nm as shown in Fig. 3. It occurs due to the electron transitions from the valence band to the conduction band in the reduction of ZnO by the phytochemicals. Then, it decreases from this inflection
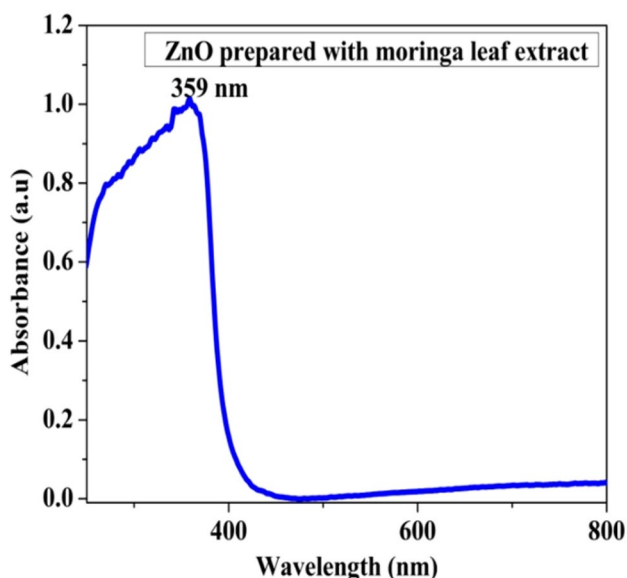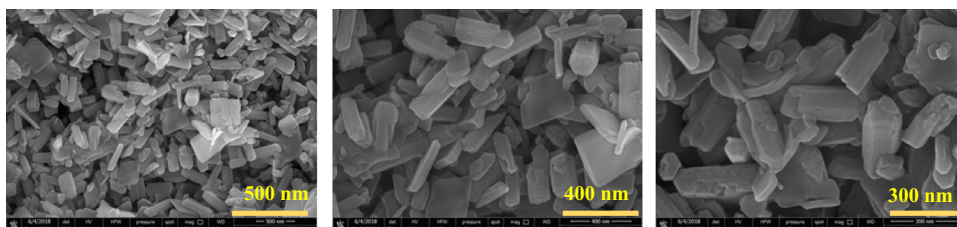

Fig. 3 UV–Visible Spectroscopy of biologically synthesized ZnO-NPs

point which is equivalent to 3.18 eV. This value is in good agreement with the bandgap of ZnO, and hence the purity and the single-phase nature of the biosynthesized ZnO-NPs obtained after annealing at 400 °C [35, 36, and 38].

10 Morphological analysis

10.1 For ZnO-NPs

FESEM micrographs of 400 °C calcined biologically synthesized ZnO-NPs is shown in Fig. 4. The morphology comprises hexagonal rods and thin plate-like structures [37, 39]. The average diameter of the hexagonal structure and rods was found to be 150–200 nm and 40 nm, respectively.

10.2 Paper

FESEM image shows an entwined network of cellulose fibers with a damaged surface, probably due to the process carried out while manufacturing the papers. The morphology of bare paper is shown in Fig. 5A. The higher magnification images obtained from the FESEM of coated samples showed the petals of a flower-like structure, which confirms the coating of ZnO-NPs on the surface of the cellulose fibers as seen in Fig. 5D and G. The hydroxyl groups on the cellulose fibers surface engage with Zn^{2+} ions to produce a Zn-O-Cellulose bonding. As a result, ZnO nuclei were created on the surface of cellulose fibers. This was further affirmed by the FESEM-based observation of ZnO-NPs [28, 40, 41].

10.3 Wood

It is known that wood inherently possesses heterogeneous and irregular surfaces, which was observed in Fig. 5B. The incorporation of ZnO-NPs on the surface of the wood substrate generates secondary roughness,

Fig. 4 FESEM image of biologically synthesized ZnO NPs

Fig. 5 A–C: FESEM Micrographs of un-coated/bare paper, wood and fabric; **D–F** FESEM micrographs of ZnO-NPs coated paper, wood and fabric in the presence of oil as an organic binder; H–I FESEM micrographs of ZnO-NPs coated paper, wood and fabric in the presence of varnish as a quasi-binder
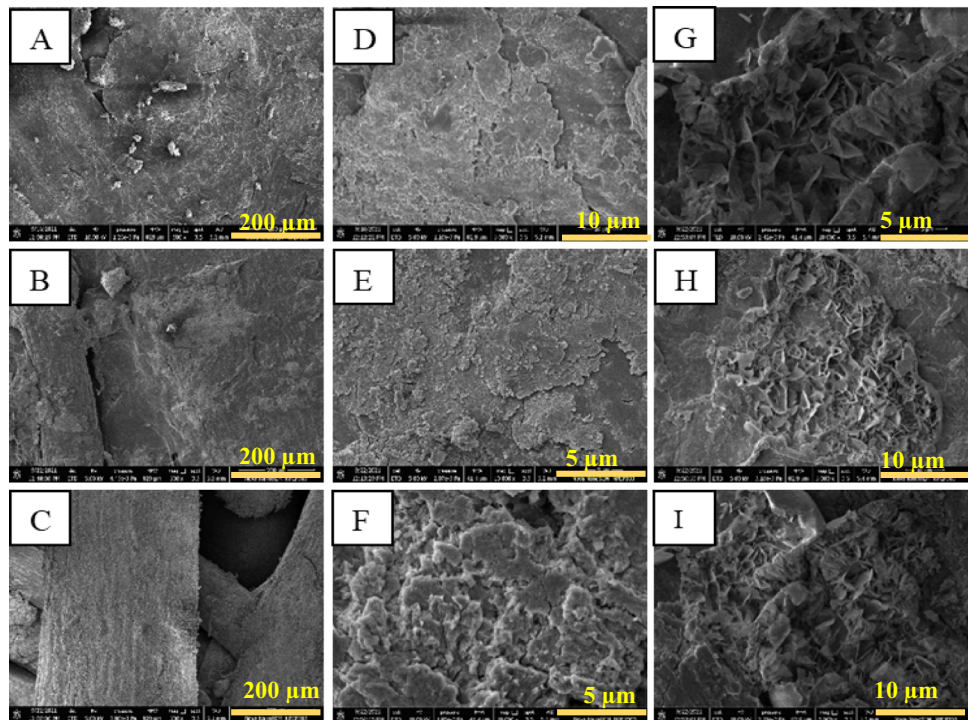
as observed in Fig. 5E H, which can contribute to the enhancement of the mechanical properties of the coated samples. According to a FESEM analysis, the presence of nano-fillers and binder traces in the cell wall and lumen of wood suggested that these heterogeneous elements had been impregnated into the wood. Due to the addition of ZnO, a binder-material matrix, the greatest improvement in flame retardancy and mechanical stability was observed [26, 27].

10.4 Fabric

The FESEM micrographs of fibers before and after coating with ZnO-NPs are shown in Fig. 5C, F and I, respectively. The smooth structure of the fabric reveals the bare sample, i.e., the sample without coating with NPs. After dip coating, a layer of NPs is observed on the fabric's surface, as shown in Fig. 5F and I, in the presence of two different binders. The fabric was submerged in a colloidal ZnO-NPs solution during the dip coating. The images demonstrated that ZnO-NP deposition produced a rough surface with a hierarchical structure. Green synthesis enhanced the adsorption of ZnO-NPs on the surface of cotton fabric, which led to the coating being caused by the physical adsorption of the NPs on the substrate. The binder firmly affixes NPs on the fabric surface. The emulsion of binders

with the NPs ensures that the coating has enough NPs and thus the effect of NPs can be observed clearly on the mechanical properties of the substrates [29, 30].

11 Thermal and mechanical properties

The 2D bare (non-coated) substrates of the present study, P and F, were dipped in oil and varnish before coating with ZnO NPs. Both Oil and varnish are flammable and volatile solvents. Hence the after-flame and after-glow values of P, and F dipped in oil and varnish took more time than bare substrates, i.e., 7, 33% in the case of paper and 7, 18% in the case of fabric.

The after-glow time for P and F showed lower values than after-flame. This is because of the property of the binders, which are flammable. The after-flame and after-glow time was recorded for bare (non-coated) samples, and coated samples with and without nanoparticles were tested, as shown in Fig. 6. Reduction in the time was observed in the case of samples coated with ZnO-NPs in the presence of oil and varnish. This is an expected outcome considering that even oil and varnish are flammable. However, the presence of ZnO NPs delayed the after-flame and after-glow time in both substrates. The after-flame and after-glow time for all the alternatives tested was delayed significantly

Fig. 6 Flame retardation test performed on the paper (P) and Fabric (F) samples
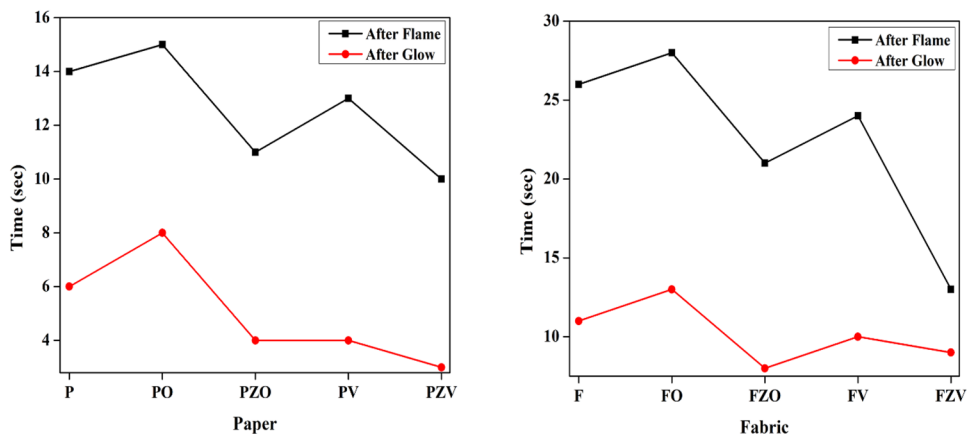
by 21, 33% in the presence of oil, 28 and 50% in the presence of varnish for paper, whereas for fabric 19, 27% in the presence of oil, 50, 18% in the presence of varnish with the addition of ZnO-NPs. The possible reason behind this could be that ZnO-nanostructured network films are intended to serve as a protective layer and endow substrates with novel functionalities. From Fig. 6, the finding implies that the ZnO-NPs arrays might serve as a thermo-protective layer, providing the underlying substrates with flame retardancy. The presence of traces of the nanofiller (NPs in this case) and the binders (polymer) in the cells of corresponding substrates indicated the impregnation of these heterogeneous materials into wood as revealed by SEM study. The significant improvement in the thermal property of P, W and F were observed in the presence of NPs with binders. The visual observations made in the wood strip provided similar results—(wood coated with the NPs delayed the after-flame and after-glow time in the presence of both binders).

Since varnish is a common sealant for wood, this is a positive outcome considering usability. Overall, the varnish binder showcased a similar range of after-flame time for all three materials, irrespective of the type of material. Varnish consists of plant-derived oils and resins with organic solvents. Although varnishes are inflammable, infusion of NPs has led to a delay in the after-glow point, increasing the material's longevity altogether.

Figure 7 shows the Tensile Strength for P, W and F. In the case of P and W, the materials are non-ductile; hence the yield point is the breakpoint showcasing ultimate tensile strength and Young's modulus. The material's tensile strength has increased in all three cases due to the ZnO-NPs. The yield point increase
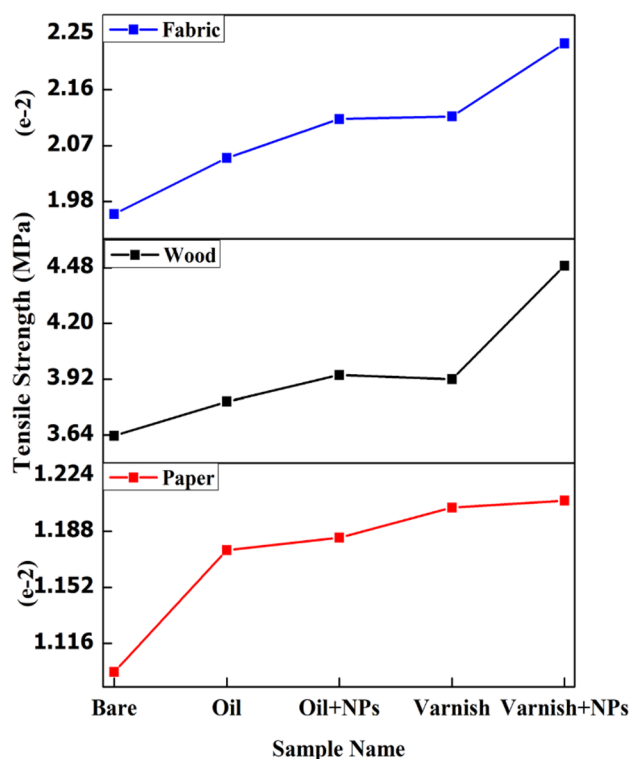

Fig. 7 Tension test result on the samples

was observed around 8% in P, W and F with ZnO-NPs and oil. The increase in yield point was observed in P, W and F as 10, 23 and 14% in the case of varnish binder with ZnO-NPs, respectively. Overall, an excellent increase in tensile strength is observed for coated samples with NPs; however, NPs with varnish showed an increase in strength his may be because the varnish hardens on drying by evaporation and due to the resins and solvents mixed into it, leading to an increase in tensile strength as that of ZnO-NPs with oil. Since

Table 1 Flame retardation and Mechanical test performed on bare and coated samples

Sample name	Mechanical property	Thermal property	
	Tensile strength (MPa)	After flame (sec)	After glow (sec)
Bare paper	0.0109	14	6
Bare wood	3.6373	–	–
Bare fabric	0.0196	26	11
Paper + oil	0.0117	15	8
Wood + oil	3.8080	–	–
Fabric + oil	0.0205	28	13
Paper + oil + NPs	0.0118	11	4
Wood + oil + NPs	3.9413	–	–
Fabric + oil + NPs	0.0211	21	8
Paper + varnish	0.0120	13	4
Wood + varnish	3.9201	–	–
Fabric + varnish	0.0212	24	10
Paper + varnish + NPs	0.0121	10	3
Wood + varnish + NPs	4.4906	–	–
Fabric + varnish + NPs	0.0223	13	9

oil is absorbed into the pores, a slight improvement in the tensile strength is observed. The possible reason would be oil penetrates in the pores of the wood, and varnish forms a protective outer layer on the surface.

However, the enhancement is less in the case of oil as though it has a lubricant nature; it offers no resistance to friction than that of varnish. In the case of varnish, it covers the material like a solid cast and upholds the substrate better in friction and under tension more effectively.

The observation of thermal property and mechanical properties in terms of tensile strength, and flame delay time after coating with different binders of all three substrates has been tabulated in Table 1.

12 Conclusion

The ZnO-NPs were successfully synthesized using *Moringa oleifera* extract and calcined at 400 °C. From XRD analysis, the pure wurtzite ZnO phase was formed with a crystallite size of 28 nm. The UV–Vis absorption wavelength of ZnO-NPs is in the UV region, and this finding suggests that the ZnO-NPs coated substrates help in retarding the UV absorption.

From FESEM micrographs, the morphology on three different substrates confirms the coating of ZnO-NPs. Infusion of NPs on the surface of three different substrates i.e., P, W and F, has modified the mechanical property by enhancing their Young's modulus and delayed the after-glow point by increasing the longevity of the material altogether. The findings indicate that biologically synthesized ZnO-NPs can be helpful in improving the surface and texture of fabricated industrial products. This can be useful for paper, pulp mill, and textile industries because their quality, standards, and regulation must be maintained before manufacturing. The ZnO-NPs enhanced the property of the substrate through the organic and quasi-organic mediums. This study has opened avenues towards enhancing the properties of NPs with binders for industrial applications of suitable substrates. All the samples showed significant rise in tensile strength due to coating alone. The tensile strength increased by 7, 5 and 5% for paper, wood and fabric in oil binder as compared to bare substrate. The strength was further augmented with the addition of nanoparticles in the presence of the binders 8, 8 and 8% with ZnO NPs addition.

Similarly, in the presence of varnish, the strength gain observed for paper, wood and fabric was 9, 8 and 8%. With NPs it increased to 10, 23 and 14% with nanoparticle addition. The highest tensile strength out of the given substrate was that of fabric as it is made up of cellulose which consists of strong hydrogen bonds attached to OH molecules, making it stiff and rigid. The cellulose is hydrophilic and has a lesser affinity towards oil, making the bond strong and unaffected.

Future Scope: Visually, the wood sample showcased delayed after-flame time and reduced after-glow time, yet accurate scientific data is in progress. The future scope of the current work can be to explore the commercialization of this work.

Author contribution

Conceptualization, ASD, VD and NB; methodology, ASD, VD and NB; software, ASD, AA and HP; validation, NB, HP and BP; formal analysis, ASD, AA, VD, NB, and BP; investigation, ASD, NB, AA and VD; resources, NB, HP and BP; data curation, ASD, NB, and VD; writing—original draft preparation, ASD, NB, AA, VD and BP; visualization, ASD, VD and NB; supervision, NB; project administration, NB; All

authors have read and agreed to the published version of the manuscript.

Data availability

The authors declare that the data supporting the findings of this study are available within the paper.

Declarations

Conflict of interest The authors hereby declare that there is no conflict of interest between us.

References

1. E. Inshakova, A. Inshakova, A. Goncharov, presented at the IOP Conference Series: Materials Science and Engineering, 2020

2. S. Davis, Trends Biotechnol. **15**(6), 217–224 (1997). https://doi.org/10.1016/S0167-7799(97)01036-6

3. N.Z. Janković, D.L. Plata, Environ. Science: Nano. **6**(9), 2697–2711 (2019). https://doi.org/10.1039/C9EN00322C

4. A.S. Desai, A. Singh, Z. Edis, S. Haj Bloukh, P. Shah, B. Pandey, N. Agrawal, N. Bhagat, J. Funct. Biomaterials. **13**(2), 54 (2022). https://doi.org/10.3390/jfb13020054

5. E.R. Sadiku, O. Agboola, M.J. Mochane, V.O. Fasiku, S.J. Owonubi, I.D. Ibrahim, B.R. Abbavaram, W.K. Kupolati, T. Jayaramudu, C.A. Uwa, *Research Anthology on Military and Defense Applications, Utilization, Education, and Ethics* (IGI Global, 2021), pp. 323–356

6. S.A. Abdel-Gawad, W.M. Osman, A.M. Fekry, Surf. Interfaces. **14**, 314–323 (2019). https://doi.org/10.1016/j.surfin.2018.08.001

7. G. Maduraiveeran, M. Sasidharan, V. Ganesan, Biosens. Bioelectron. **103**, 113–129 (2018). https://doi.org/10.1016/j.bios.2017.12.031

8. S. Otles, B.Y. Şahyar, *Nanotechnology Applications in the Food Industry* (CRC Press, Boca Raton, 2018), pp.97–106

9. W. Chen, H. Chen, W. Li, J. Huang, J. Yu, J. Duh, S. Lan, T. Feng, Surf. Coat. Technol. **389**, 12563610 (2020)

10. P.C. Ray, H. Yu, P.P. Fu, J. Environ. Sci. Health Part C **27**(1), 1–35 (2009). https://doi.org/10.1080/10590500802708267

11. I. Khan, K. Saeed, I. Khan, Arab. J. Chem. **12**(7), 908–931 (2019). https://doi.org/10.1016/j.arabjc.2017.05.011

12. F. Pacheco-Torgal, S. Jalali, Constr. Build. Mater. **25**(2), 582–590 (2011). https://doi.org/10.1016/j.conbuildmat.2010.07.009

13. H. Duan, D. Wang, Y. Li, Chem. Soc. Rev. **44**(16), 5778–5792 (2015). https://doi.org/10.1039/C4CS00363B

14. K.N. Thakkar, S.S. Mhatre, R.Y. Parikh, Nanomed.: Nanotechnol., Biol. Med. 6 (2), 257–262 (2010).

15. A. Husen, M. Iqbal, *Nanomaterials and Plant Potential: An Overview* (Springer, Amsterdam, 2019)

16. A. Sirelkhatim, S. Mahmud, A. Seeni, N.H.M. Kaus, L.C. Ann, S.K.M. Bakhori, H. Hasan, D. Mohamad, Nano-micro Lett. **7**, 219–242 (2015). https://doi.org/10.1007/s40820-015-0040-x

17. A.N. Papadopoulos, H.R. Taghiyari, Coatings. **9**(12), 866 (2019). https://doi.org/10.3390/coatings9120866

18. C.H. Suh, Y.-C. Jung, Y.S. Kim, J. Mech. Sci. Technol. **24**, 2091–2098 (2010). https://doi.org/10.1007/s12206-010-0707-7

19. I. Perelshtein, G. Applerot, N. Perkas, G. Guibert, S. Mikhailov, A. Gedanken, Nanotechnology. **19**(24), 245705 (2008). https://doi.org/10.1088/0957-4484/19/24/245705

20. Y.A. Molina, V.R. Tapia, E.B. Calva, Plasmonics. **11**, 971–979 (2016). https://doi.org/10.1007/s11468-015-0131-z

21. A. Mathiazhagan, R. Joseph, Int. J. Chem. Eng. Appl. **2**(4), 225 (2011)

22. Y. Wong, C. Yuen, M. Leung, S. Ku, H. Lam, AUTEX Res. J. **6**(1), 1–8 (2006)

23. R. Olar, Buletinul Institutului Politehnic din Iasi. Sectia Constructii, Arhitectura. **57**(4), 109 (2011)

24. M.J. Hanus, A.T. Harris, Prog. Mater. Sci. **58**(7), 1056–1102 (2013). https://doi.org/10.1016/j.pmatsci.2013.04.001

25. V.S. Chauhan, S.K. Chakrabarti, Cellul. Chem. Technol. **46**(5), 389 (2012)

26. R.R. Devi, T.K. Maji, Wood Sci. Technol. **47**, 1135–1152 (2013). https://doi.org/10.1007/s00226-013-0563-6

27. H.J. Seo, S. Kim, W. Huh, K.-W. Park, D.R. Lee, D.W. Son, Y.-S. Kim, J. Therm. Anal. Calorim. **123**, 1935–1942 (2016). https://doi.org/10.1007/s10973-015-4553-9

28. R.R.A. Hassan, W.S. Mohamed, Appl. Phys. A **124**, 1–10 (2018). https://doi.org/10.1007/s00339-018-1989-3

29. N.F. Attia, M. Moussa, A.M. Sheta, R. Taha, H. Gamal, Prog. Org. Coat. **104**, 72–80 (2017). https://doi.org/10.1016/j.porgcoat.2016.12.007

30. I.S. Tania, M. Ali, Polymers. **13**(16), 2701 (2021). https://doi.org/10.3390/polym13162701

31. N. Bhagat, B. Pandey, Curr. Nanosci. **18**(6), 726–732 (2022). https://doi.org/10.2174/1573413717666211118105842

32. P. Scherrer, Nach Ges Wiss Gottingen. **2**, 8–100 (1918)

33. J.I. Langford, A. Wilson, J. Appl. Crystallogr. **11**(2), 102–113 (1978). https://doi.org/10.1107/S0021889878012844

34. V. Uvarov, I. Popov, Mater. Charact. **85**, 111–123 (2013). https://doi.org/10.1016/j.matchar.2013.09.002

35. S. Saif, A. Tahir, T. Asim, Y. Chen, M. Khan, S.F. Adil, Saudi J. Biol. Sci. **26**(7), 1364–1371 (2019). https://doi.org/10.1016/j.sjbs.2019.01.004

36. N. Matinise, X. Fuku, K. Kaviyarasu, N. Mayedwa, M. Maaza, Appl. Surf. Sci. **406**, 339–347 (2017). https://doi.org/10.1016/j.apsusc.2017.01.219

37. J. Akintunde, T. Farai, M. Arogundade, J. Adeleke, Biochem. Biophys. Rep. **26**, 100999 (2021). https://doi.org/10.1016/j.bbrep.2021.100999

38. S. Pal, S. Mondal, J. Maity, R. Mukherjee, Int. J. Nanosci. Nanatechnol. **14**(2), 111–119 (2018)

39. H.G. Yang, H.C. Zeng, J. Phys. Chem. B **108**(11), 3492–3495 (2004). https://doi.org/10.1021/jp0377782

40. O.M. El-Feky, E.A. Hassan, S.M. Fadel, M.L. Hassan, J. Cult. Herit. **15**(2), 165–172 (2014). https://doi.org/10.1016/j.culher.2013.01.012

41. I. Chauhan, S. Aggrawal, P. Mohanty, Environ. Science: Nano. **2**(3), 273–279 (2015). https://doi.org/10.1039/C5EN00006H

Publisher's Note Springer Nature remains neutral with regard to jurisdictional claims in published maps and institutional affiliations.